Experiments in Navigation and Mapping with a Hovering AUV

George Kantor, Nathaniel Fairfield, Dominic Jonak and David Wettergreen
The Robotics Institute
Carnegie Mellon University
Pittsburgh, Pennsylvania 15213 USA
Email: {kantor, than, dom, dsw}@cmu.edu

May 31, 2007

Abstract

This paper describes the basic control, navigation, and mapping methods and experiments a hovering autonomous underwater vehicle (AUV) designed to explore flooded cenotes in Mexico as part of the DEPTHX project. We describe the low level control system of the vehicle, and present a dead reckoning navigation filter that compensates for frequent Doppler velocity log (DVL) dropouts. Sonar data collected during autonomous excursions in a limestone quarry are used to generate a map of the quarry geometry.

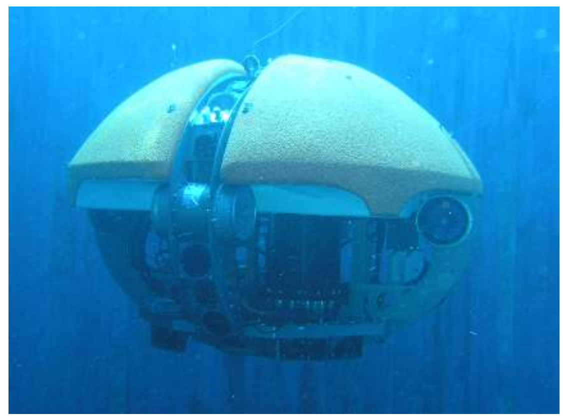

Figure 1: The DEPTHX AUV Clementine deployed in a test tank at Austin Research Laboratory.

1 Introduction

The DEPTHX (DEep Phreatic THermal eXplorer) project is a three-year NASA-funded effort whose primary objective is to use an autonomous vehicle to explore and characterize the unique biology of the Zacatón cenote. Zacatón, the world's deepest known limestone sinkhole, is a water-filled cavern that is at least 300 meters deep. The depths of Zacatón are geothermally heated with a high sulfur content and a lack of sunlight or dissolved oxygen, making this an ideal place to search for exotic microbial life (Gary 2002). The robotic exploration and search for microbial life in Zacatón is an analog mission for the search for life in the liquid water ocean beneath the frozen surface of Europa.

The DEPTHX robot (Figure 1) is a hovering autonomous underwater vehicle (AUV) designed to explore flooded caverns and tunnels while building 3D maps, collecting environmental data, and obtaining samples from the water column and cavern walls. To accomplish these tasks, the vehicle is equipped with a Doppler velocity logger (DVL), a ring laser gyro-based inertial navigation system (INS), a depth sensor, and an array of 54 narrow beam sonar transducers. In the Zacatón mission, the vehicle will use all of these sensors together to perform simultaneous localization and mapping (SLAM). This paper presents a preliminary field result where the INS, DVL, and depth sensor are used together to generate a dead reckoned position estimate and the sonar array is used to create a map based on that estimate. This technique was used to autonomously map a limestone quarry in Austin, Texas during field tests conducted in January of 2007.

The paper is organized as follows: Related research activities in using AUVs for science and mapping are briefly discussed in Section 2. Then we provide a description of the instrumentation of the DEPTHX vehicle in Section 3. This is followed by a description of our implementation of a Kalman filter to merge DVL and IMU measurements, allowing for high performance dead reckoned position estimation even in cases where the DVL frequently drops out (Section 4). An overview of the vehicle control system is provided in Section 5. Experimental results are presented in Section 7, followed by some conclusions and a discussion of future work in Section 8.

2 Related Work

There are more than 1000 commercial underwater vehicles in operation today, performing tasks as diverse as archaeological excavation to drill-rig maintenance to oceanographic survey (Whitcomb 2000).

There are a variety of techniques employed for determining the position of underwater vehicles – unfortunately GPS does not work underwater – and they can be divided into those that utilize emplaced infrastructure and those that do not. (See Leonard et al. (1998) for a comprehensive survey.)

When accurate position is needed underwater, most AUVs and many human-driven remotely operated vehicles (ROVs) rely on a surveyed array of acoustic beacons, known as a long base-line (LBL) array. Acoustic beacons provide a fixed frame of reference for positioning the vehicle (Whitcomb 2000). Yoerger et al. (2007) have shown detailed sea-floor mapping of subsea vents using an LBL array with the Autonomous Benthic Explorer.

Over large distances, or in underwater caves and tunnels, the performance of LBL systems is unknown due to signal attenuation, reverberation and multipath. Without a fixed LBL infrastructure, an AUV uses a combination of depth sensors, inertial sensors, and Doppler velocity sensors to compute a dead reckoned estimate of its position while at depth. With high accuracy attitude and depth sensors the uncertainty in the AUV's 3D pose (roll, pitch, yaw, x, y, z) is primarily in x and y. Most underwater navigation systems are based on a Kalman Filter which combines Doppler velocity and inertial measurements (Larsen 2000). These systems report navigation errors as low as 0.015% of distance traveled, however error accrues drastically in situations where the DVL is unable to make accurate velocity measurements. Kirkwood et al. (2001) have developed an AUV for multi-day under-ice arctic survey.

Eventually the dead reckoned estimate will drift from true, and when the accumulated error exceeds what is required for the application, a correction must be made by (re)observing a known reference. A common approach is to surface and obtain position from a GPS. If LBL or surfacing is not an option, the position error can be bounded by simultaneous localization and mapping (SLAM) (Williams et al. 2000) (Dissanayake et al. 2001). (Williams and Mahon 2004) provide an example of near-bottom mapping with sonars and cameras of coral reefs using SLAM. Roman (2005) uses multibeam sonar maps to do SLAM over varied topography.

3 Vehicle Description

The DEPTHX vehicle is a hovering AUV that has been specifically designed for exploration of flooded caverns and tunnels. It has an ellipsoidal shape that measures approximately 1.5 meters in height and 1.9 meters in both length and width (Figure 2). Its dry mass is 1500kg. Four large pieces of syntactic foam are mounted on the top half of the vehicle, passively stabilizing the vehicle roll and pitch. The vehicle can move directly in the remaining four degrees of freedom (forward, starboard, down, and heading) using six thrusters driven by brushless DC motors. The cruising speed of the vehicle is about 0.2 meters per second. The vehicle is powered by two 56-volt Lithium-Ion battery stacks with a total capacity of 6.2 KWh, enough to supply the vehicle during an four-hour exploration mission.

The DEPTHX vehicle has a full suite of underwater navigation sensors, including a Honeywell HG2001AC INS, two Paroscientific Digiquartz depth sensors, and an RDI Navigator 600kHz DVL. The two depth sensors are tared, or zeroed with respect to atmospheric pressure, at the start of each

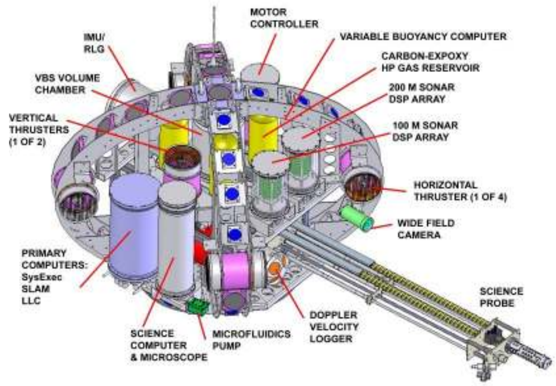

Figure 2: A model of the DEPTHX vehicle structure and components. Eleven pressure vessels house computing, batteries, sensors, and science instruments. Diameter is approximately 2m. ©Stone Aerospace, 2006.

day. The DVL is mounted to the front of the vehicle facing forward and tilted down 30 degrees from horizontal, a nonstandard configuration for this instrument. The usual DVL configuration points straight down so that it can achieve lock on the ocean floor. In our application, it is difficult to predict the relative direction to surfaces useful for DVL lock. The top 280 meters of Zacatón is known to be a chimney with a diameter of approximately 80 meters (Fairfield et al. 2005), so the forward-looking configuration should allow the DVL to lock on to one of the vertical walls in most situations. This configuration can cause the DVL to lose bottom lock in more wide-open waters, such as the quarry that is the subject of this paper. Loss of bottom lock can also occur at extremely short ranges, or when passing over highly irregular terrain.

For our purposes, the raw roll, pitch, and yaw measurements provided by the IMU and the depth measurements provided by the depth sensors are accurate enough to be considered absolute measurements of those quantities. The task of determining the location of the vehicle is then reduced to the two dimensional problem of estimating its position in the lateral plane (x and y).

For mapping, the vehicle has an array of 54 2° beam-width sonars that provide a constellation of range measurements around the vehicle. This array is in the shape of three great circles, a configuration that was arrived at after studying the suitability of various sonar geometries for the purposes of SLAM (Fairfield et al. 2005). The sonars have long ranges (some 100m and others 200m) and the accuracy of the range measurements is fairly high (about 10cm), however the low resolution, update rate, and point density makes the mapping problem significantly more difficult than it is with ranging sensors like a laser scanner that provide fast, accurate, high-resolution range images.

4 Dead Reckoning Localization

The concept of dead reckoning from DVL velocities is straightforward: integrate the velocities to obtain a position estimate. Here we lay out the details of how this is done on the DEPTHX vehicle.

4.1 Dead Reckoning with DVL Velocities

The raw DVL measurement is a vector specifying the velocity of the DVL in the DVL's own coordinate frame. Using the notation of Spong et al. (2006), we denote this vector by $\mathbf{v}_{dvl}^{dvl}$. We actually want to know the velocity of the origin of the vehicle frame (which is located at the centroid of the vehicle) represented in the world frame, which we denote by $\mathbf{v}_v^w$. To get this, we first compute the velocity of the vehicle in the vehicle frame:

$$\mathbf{v}_v^v = R_{dvl}^v \mathbf{v}_{dvl}^{dvl} - \omega_v^v \times \mathbf{o}^{dvl}.$$

Here, R_{dvl}^v is the constant rotation matrix describing the orientation of the DVL relative to the vehicle frame; $\omega_v^v = [\omega_x \ \omega_y \ \omega_z]^T$ are the angular velocities in vehicle frame (as measured by the IMU); and $\mathbf{o}^{dvl}$ is the position of the DVL in the vehicle frame (or lever-arm.) It is then a simple matter to rotate the vehicle frame velocities into the world frame

$$\mathbf{v}_v^w = R_v^w \mathbf{v}_v^v,$$

where R_v^w is the rotation matrix describing the orientation of the vehicle relative to the world frame, as measured by the IMU. The x and y components of $\mathbf{v}_v^w$ are then numerically integrated to get the new dead reckoned x and y position estimates using Euler's method.

4.2 Patching DVL Dropouts

As discussed above, the forward-looking configuration of the DVL together with uneven bottom conditions causes it to frequently lose bottom lock in open water situations. During these times, no DVL velocity measurements are available, making it impossible to update the dead reckoned position estimate. Another unfortunate symptom of losing bottom lock is that the last few DVL measurements before and the first few measurements after the loss of lock are likely to be noisy. In order to filter out these measurements, we used a simple first difference filter to discard DVL measurements which indicated a change in speed of more that 0.05 m/s – the vehicle does not have a very high acceleration.

Our approach to solving this dropout problem involves using the velocity estimates provided by the IMU to continue the dead reckoning solution when DVL measurements are unavailable. However, since the IMU velocity estimates result from integrating measurements from the IMU accelerometers, they are subject to significant drift. To address this problem, we use a Kalman filter to estimate the drift of the IMU velocity estimates during the times when the DVL measurements are good (i.e., when the DVL has a lock).

We implement this with two independent and identical Kalman filters. One filter is used to estimate the IMU velocity and drift in the world frame x direction, the other is used to estimate the same parameters in the y direction. The state of each filter is $q = [v,\ d]^T$, where v is the world frame vehicle velocity in the relevant direction, and d is the associated IMU drift term. If we define q_k to be the value of the state at the time t and q_{k+1} to be the value of the state at the time $t + \Delta t$, then the state transition model that maps (q_k, a_k) to q_{k+1} is

$$q_{k+1} = \begin{bmatrix} 1 & \Delta t \\ 0 & 1 \end{bmatrix} q_k + \begin{bmatrix} 1 \\ 0 \end{bmatrix} a_k + w_k \triangleq F_k q_k + G a_k + w_k,$$

where the process noise w_k is assumed to be white, zero-mean, and Gaussian with covariance matrix Q. The DVL provides a measurement of the velocity v, so the measurement model is

$$y_k = \begin{bmatrix} 1 & 0 \end{bmatrix} q_k + \nu_k \triangleq H_k q_k + \nu_k,$$

where the measurement noise ν_k is assumed to be white, zero-mean, and Gaussian with variance R. From here, the filter is implemented using the standard Kalman equations (see, e.g., (Maybeck 1979)), with the small caveat that prediction steps are executed whenever an IMU measurement is received (about 50 Hz) and update steps are executed whenever a valid DVL measurement is received (about 4 Hz).

5 Vehicle Controller

The DEPTHX vehicle has a three-level control system that is used to guide the vehicle on its mission. The lowest level, aptly named the low level control system (LLCS), employs velocity feedback from the DVL and IMU in order to generate the thrust necessary to track a desired vehicle frame velocity command. The middle level, named the navigator, issues velocity commands to the LLCS in order to achieve the immediate goal. In this paper, the immediate goal is to drive the vehicle to a specified waypoint, however the navigator also is capable of executing more general behaviors such as wall following and obstacle avoidance. At the highest level is the system executive that, among other things, issues a series waypoint commands to the navigator in order to accomplish the overall mission.

5.1 Low Level Control System

The LLCS performs two basic functions: it uses velocity feedback to convert a vehicle frame velocity command into the vehicle frame thrust needed to track that velocity and it implements a mixing table in order to convert the vehicle frame thrust command into the necessary shaft torque [1] commands to each of the individual thrusters.

Velocity feedback is implemented in four independent loops, one for each of the vehicle's four degrees of freedom. Each loop contains an experimentally tuned PI controller. Note that this structure

[1] The relationship between shaft torque and thrust is very nearly linear, and we rely on the DriveBlok^{TM} controller produced by MTS Systems Corp to implement the desired shaft torque on the brushless DC thruster motors.

assumes that the components of vehicle frame velocity are not coupled by the dynamics of the vehicle, an assumption which not true. In particular, the forward and sideways velocity components of the vehicle will be highly coupled when the vehicle simultaneously rotates and moves in the lateral plane. Hence we can enforce the decoupled assumption by simply avoiding these type of motions, a restriction which is compatible with the slow, deliberate types of missions that the vehicle will undertake. In practice, however, the controller performs well even when such coupling motions are executed.

The thrust mixer maps the vehicle frame thrust command vector $F_v = [F_\omega, F_x, F_y, F_z]^T$ into a vector of n individual thruster commands $T = [\tau_1, \tau_2, \tau_3, \ldots, \tau_n]^T$, where n is the number of thrusters. It is implemented as a matrix multiplication, i.e., $T = MF_v$, where M is computed as follows. First, let A be the $6 \times n$ matrix whose ith column is given by

$$A_i = \begin{bmatrix} p_i \times D_i \\ D_i \end{bmatrix},$$

where p_i is a vector describing the location of the ith thruster in the vehicle frame, and D_i is a vector describing the positive thrust direction of the ith thruster in the vehicle frame. Now let B be the $4 \times n$ matrix that is the bottom four rows of A. B is the matrix that maps the individual thruster thrusts T into the resulting vehicle frame thrust vector F_v. Assuming that the rows of B are linearly independent, M can then be found by taking the pseudoinverse of B:

$$M = B^T \left(BB^T\right)^{-1}.$$

Note that in the nominal case, the number of thrusters is $n = 6$. However, this formulation allows the mixing matrix to easily be recomputed in the event of thruster failure.

6 Mapping

In the DEPTHX mission to Zacatón, the vehicle will employ a sophisticated SLAM system that uses 3D evidence grids as maps and uses a Rao-Blackwellized particle filter to simultaneously estimate the most likely combination vehicle trajectory

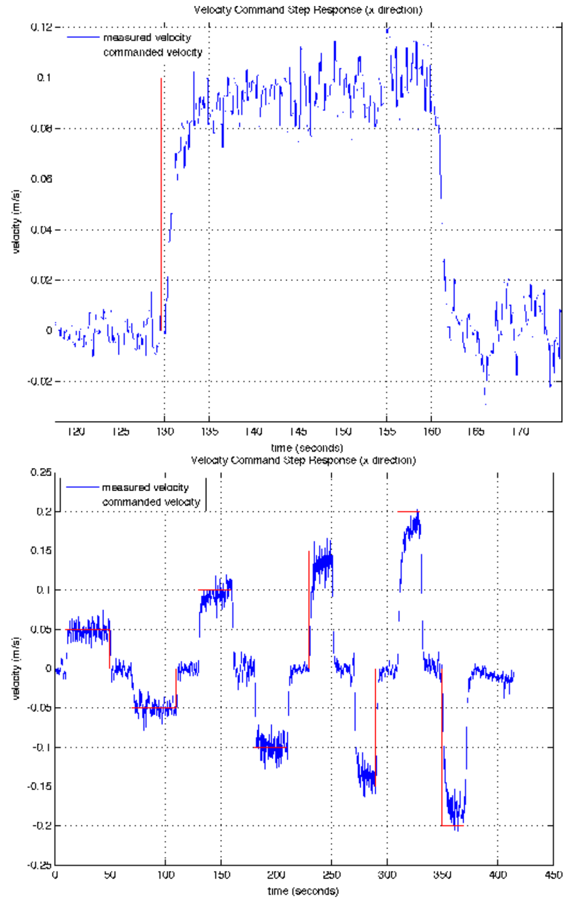

Figure 3: Velocity tracking performance of the LLCS for various commanded velocity pulses. The duration of the leading and falling edge transients is on the order of 4 seconds.

and world map (Fairfield et al. 2007). In this paper, we present a simplistic method of generating a map of an explored area. Namely, we assume that the dead reckoned position estimate described above is correct and we use that estimate to determine the locations of points on the quarry walls sensed by the array of mapping sonars. By manually using GPS to measure the starting location of the vehicle, the resulting map can be registered into UTM coordinates. The details of our implementation of this process are described here.

First, the dead reckoned position estimate is combined with the IMU roll, pitch, and yaw measurements and the depth sensor measurement to generate a full 6-DOF pose estimate for the vehicle. This is represented by the homogeneous transformation matrix H_v^w. We also represent the pose of each mapping sonar relative to the vehicle frame as a homogeneous transformation matrix. Specifically, H_{si}^v describes the 6-DOF pose of the ith sonar transducer relative to the vehicle frame. These matrices are constant and computed in advance. The sonar coordinate frames are defined such that the x axis is aligned with the axis of the sonar beam. So given a sonar range measurement r_i, we can compute the world frame location of the sensed point as

$$\begin{bmatrix} p_i^w \\ 1 \end{bmatrix} = H_v^w H_{si}^v \begin{bmatrix} r_i \\ 0 \\ 0 \\ 1 \end{bmatrix}.$$

With this relationship, the mapping process is simply a matter of driving in a survey pattern while maintaining the vehicle pose estimate and computing the points p_i^w as the sonar range measurements are received. These points are filtered to eliminate surface reflections and other noise. Below, we describe building a simple map from the point cloud data.

We can then insert the sonar point cloud into a kd-tree (Bentley 1975), and use the ANN library (Mount and Arya 1997) to implement a simple weighted k-nearest neighbor algorithm to build a regularly sampled map.

7 Experimental Results

7.1 LLCS Results

The plots in Figure 3 demonstrate the typical performance we have observed for the low level control system. The vehicle tracks velocity commands well after a transient period of about 4 seconds. This performance should be sufficient to execute the anticipated DEPTHX missions.

7.2 Dead Reckoning Results

Figure 4 shows the performance of the dead reckoning system described in Section 4 during a long raster mission to map the quarry. This mission had a total path length of over a kilometer, at the end of which the positioning error was 3.16 meters. This gives a respectable dead reckoning accuracy of less than half a percent of distance traveled. It should be noted that GPS fixes used as ground truth in this experiment were taken using a hand held non-differential GPS receiver from a moving boat, so it is likely that the dead reckoning estimate is actually more accurate than the “ground truth”.

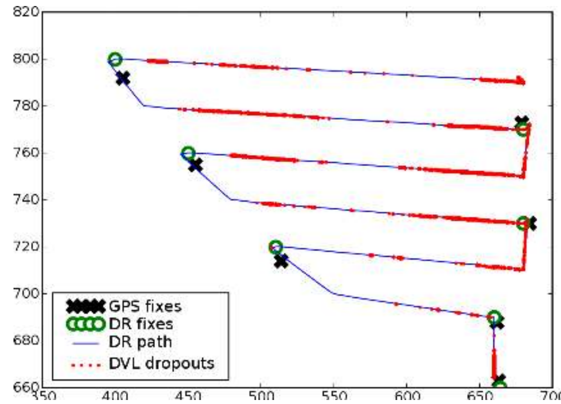

Figure 4: Dead reckoning localization performance over raster scan mission of quarry.

The red dots in Figure 4 denote locations where the DVL failed to achieve bottom lock. During this 6300 second mission, the vehicle was without DVL measurements for a total of about 780 seconds. Some of these dropout periods were as long as sixty seconds. Given this DVL performance, it would have been impossible to achieve any sort of dead reckoning estimate without patching in the IMU velocities as estimated by the Kalman filter.

7.3 Mapping Results

In order to produce a map of the quarry, the vehicle performed several overlapping survey missions, designed to provide sonar converage of all the navigable regions of the quarry. We then concantenated all the data points from these missions, and used the nearest-neighbor approach described above to build the regularly sampled map shown in Figure 5.

8 Conclusions and Future Work

This paper demonstrates the most basic capabilities of the DEPTHX vehicle, a hovering AUV designed

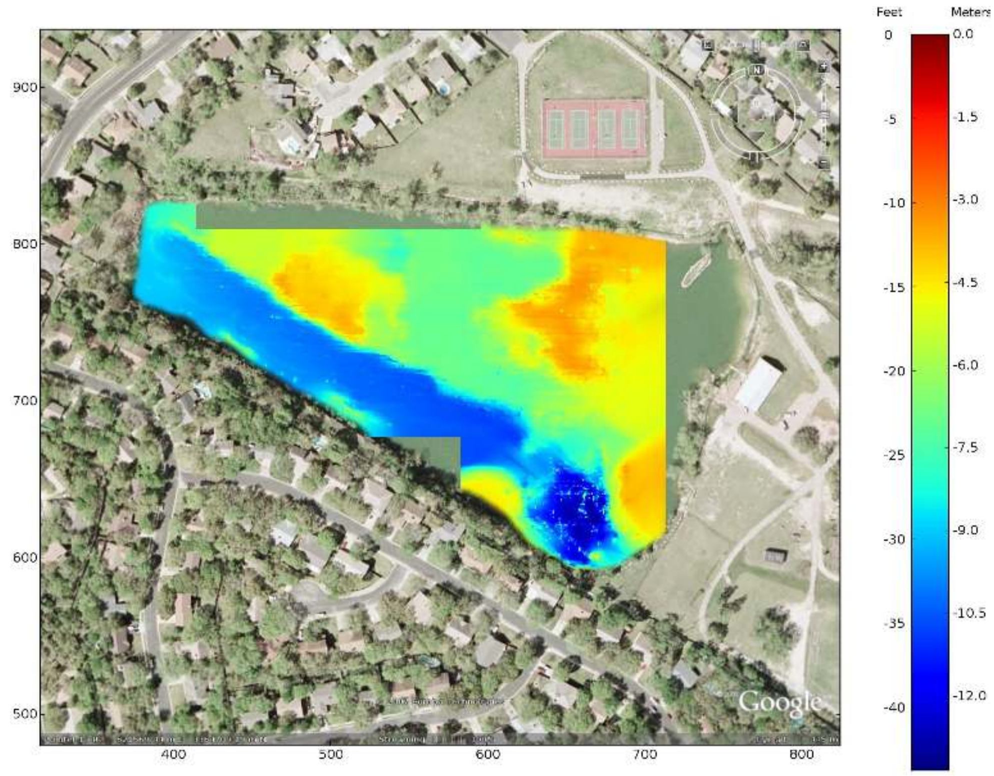

Figure 5: A map of quarry geometry generated using weighted k-nearest neighbor interpolation. Background image courtesy Google, ©Europa Technologies, 2007.

to explore and map flooded cenotes in Mexico as part of the DEPTHX project. We have demonstrated the ability to do basic motion control, achieve decent position estimates from dead reckoning with unreliable DVL data, and use the mapping sonars to generate a map. During the first half of 2007, more sophisticated capabilities will be developed and tested in a series of missions to the La Pilita and Zacatón cenotes in central Mexico. These abilities include more sophisticated motion control, including the ability to maneuver in close proximity along the cavern walls, scanning the walls for suitable locations to take a solid sample. In the area of localization and mapping, the vehicle will use its dead reckoned position and its sonars to build a 3D map – but it will also use this map to simultaneously localize itself, which allows the vehicle to correct for the gradual drift in the dead reckoned position. The dead reckoning capability demonstrated by our experiments in the quarry is a key element of the performance of the DEPTHX Simultaneous Localization and Mapping (SLAM) system, which is described in (Fairfield et al. 2007).

Acknowledgments

We would like to thank the Hyde Park Baptist Church in Austin, Texas for allowing us to use their quarry for two weeks of robot testing. We would also like to thank the other members of the DEPTHX team for their roles in bringing the DEPTHX vehicle together. In particular, we thank John Kerr and Bill Stone at Stone Aerospace and Marcus Gary at the Department of Geology at the University of Texas, Austin. This work was funded by the NASA ASTEP program, grant NNG04GC09G.

References

Bentley, J. (1975). Multidimensional binary search trees for associative searching. *Commun. ACM*, 18(9):509–517.

Dissanayake, G., Newman, P., Clark, S., Durrant-Whyte, H. F., and Csorba, M. (2001). A solution to the simultaneous localisation and map building (SLAM) problem. *IEEE Transactions on Robotics & Automation*, 17(3):229–241.

Fairfield, N., Kantor, G. A., and Wettergreen, D. (2005). Three dimensional evidence grids for SLAM in complex underwater environments. In *Proc. of the 14th Intl. Symposium of Unmanned Untethered Submersible Technology*.

Fairfield, N., Kantor, G. A., and Wettergreen, D. (2007). Real-time slam with octree evidence grids for exploration in underwater tunnels. *Journal of Field Robotics (to appear)*.

Gary, M. O. (2002). Understanding Zacatón: Exploration and initial interpretation of the world's deepest known phreatic sinkhole and related karst features, southern Tamaulipas, Mexico. *Karst Frontiers, Karst Waters Institute Special Publication*, 7:141–145.

Kirkwood, W., Gashler, D., Thomas, H., O'Reilly, T., McEwen, R., Tervalon, N., Shane, F., Au, D., Sibenac, M., Konvalina, T., Bahlavouni, A., and Bellingham, J. (2001). Development of a long endurance autonomous underwater vehicle for ocean science exploration. In *IEEE Oceans 2001*, pages 1504–1512.

Larsen, M. B. (2000). High performance doppler-inertial navigation experimental results. In *Proc. of IEEE/MTS OCEANS*, pages 1449–1456.

Leonard, J. J., Bennett, A. A., Smith, C. M., and Feder, H. J. S. (1998). Autonomous underwater vehicle navigation. Technical report, MIT Marine Robotics Laboratory.

Maybeck, P. S. (1979). *Stochastic models, estimation, and control*, volume 141 of *Mathematics in Science and Engineering*. Academic Press.

Mount, D. and Arya, S. (1997). ANN: A library for approximate nearest neighbor searching. In *CGC 2nd Annual Fall Workshop on Computational Geometry*. available at *http://www.cs.umd.edu/mount/ANN*.

Roman, C. (2005). *Self Consistent Bathymetric Mapping from Robotic Vehicles in the Deep Ocean*. PhD thesis, Massachusetts Institute of Technology & Woods Hole Oceanographic Institution.

Spong, M. W., Hutchinson, S., and Vidyasagar, M. (2006). *Robot Modeling and Control*. John Wiley and Sons, Inc.

Whitcomb, L. (2000). Underwater robotics: Out of the research laboratory and into the field. In *IEEE 2000 International Conference on Robotics and Automation*.

Williams, S., Newman, P., Dissanayake, G., and Durrant-Whyte, H. (2000). Autonomous underwater simultaneous localisation and map building. In *Proc of IEEE Conf. on Robotics and Automation*.

Williams, S. B. and Mahon, I. (2004). Simultaneous localisation and mapping on the great barrier reef. In *Proc. of IEEE Intl. Conf. on Robotics and Automation*, volume 2, pages 1771–1776.

Yoerger, D., Jakuba, M., Bradley, A., and Bingham, B. (2007). Techniques for deep sea near-bottom survey using an autonomous underwater vehicle. *International Journal of Robotics Research*, 26(1):41–54.